Dyes and Pigments 171 (2019) 107722

Contents lists available at ScienceDirect

Dyes and Pigments

journal homepage: www.elsevier.com/locate/dyepig

Development of a novel near-infrared fluorescence light-up probe with a large Stokes shift for sensing of cysteine in aqueous solution, living cells and zebrafish

Xiaoyu Zhang[a], Heng Liu[a,c,**], Yingying Ma[a], Wangbo Qu[a], Hanping He[a], Xiuhua Zhang[a], Shengfu Wang[a], Qi Sun[b,***], Fabiao Yu[c,*]

[a] Hubei Collaborative Innovation Center for Advanced Organic Chemical Materials, Ministry of Education Key Laboratory for the Synthesis and Application of Organic Functional Molecules & College of Chemistry and Chemical Engineering, Hubei University, Wuhan, 430062, China

[b] Key Laboratory for Green Chemical Process of Ministry of Education and School of Chemistry and Environmental Engineering, Wuhan Institute of Technology, Wuhan, 430205, China

[c] Institute of Functional Materials and Molecular Imaging, Key Laboratory of Emergency and Trauma, Ministry of Education, Key Laboratory of Hainan Trauma and Disaster Rescue, College of Clinical Medicine, College of Emergency and Trauma, Hainan Medical University, Haikou, 571199, China

ARTICLE INFO

Keywords:
Fluorescent probes
Near-infrared emission
Cell imaging
In vivo imaging
Cysteine

ABSTRACT

As an important sulfur-containing amino acid, aberrant levels of cysteine are closely related with an array of dieases. Although many Cys-specific fluorescent probes have been designed, most of them wouldn't be able to detect Cys in buffer solution, which limits the application of the probe in biological system. In this work, a novel near-infrared fluorescent probe Cys-WR with a large Stokes shift (about 110 nm) was developed for the detection of Cys by conjugating the fluorophore WR-4 with crotonate moiety. The probe exhibited off-on response to Cys with wide linear range of 0–100 μM, as well as the color of the probe solution changes from deep pink to brown observed by naked eyes. Moreover, the probe showed little cytotoxicity. Imaging of Cys using this probe in living A549 cells and zebrafish had also been well demonstrated.

1. Introduction

Cysteine (Cys), a kind of reactive sulfur species (RSS) which contains the mercapto group, is invovled in an array of physiological and pathological functions [1–3]. Increasing available evidence suggest that aberrant changes of Cys level are implicated with a wide variety of dieases, such as liver damage, cardiovascular disease, skin lesions, Alzheimer's disease and cancer [4–6]. Consequently, the development of an efficient method for specific assessment of Cys is of great significant in the diagnosis and treatment of related diseases. In comparison with tradition analytical methods, fluorescent imaging is a more useful tool for exploring the activities of biomolecules in living cells and tissue [7–11]. Meanwhile, fluorescent probes with emission in near-infrared (NIR) range (650–900 nm) have enabled to reduce cell damage, eliminate background autofluorescence and increase the depth of tissue penetration, thereby improving imaging accuracy [12–15]. However, the chemical structure and reaction reactivity of Cys is similar to glutathione (GSH) and homocysteine (Hcy), which make specific recognition of Cys in biological systems face great challenges [16]. To solve this problem, a significant amount of small organic molecules have been used to design fluorescent probes for specific detection of Cys in the presence of GSH and Hcy in the past few years [17–27]. Unfortunately, only few Cys-specific probes can be used in the low volume ratio (below 1%) of organic solvents [28–31]. Among them, the probes that emitted in long wavelength with large Stokes shifts were rare. Thus, designing NIR fluorescent probes with large Stokes shifts for sensing of Cys in aqueous solution is still desirable.

Herein, we reported the development of a novel NIR fluorescent probe with a large Stokes shift, Cys-WR, for the determination of Cys. The probe was constructed with the fluorophore WR-4 as a fluorescent reporter and crotonate as a sensing moiety [32]. The probe showed high selectivity toward Cys over other interfering analytes in aqueous solution and would enable to visualize Cys in living cells and zebrafish.

* Corresponding author. Hainan Medical University, Haikou 571199, China.
** Corresponding author. Hubei University, Wuhan 430062, China.
*** Corresponding author Wuhan Institute of Technology, Wuhan 430205, China.
E-mail addresses: liuheng11b@hubu.edu.cn (H. Liu), qisun@wit.edu.cn (Q. Sun), fbyu@yic.ac.cn (F. Yu).

https://doi.org/10.1016/j.dyepig.2019.107722
Received 23 June 2019; Received in revised form 13 July 2019; Accepted 16 July 2019
Available online 17 July 2019
0143-7208/

2. Experimental section

2.1. Reagents and apparatus

All reagents and solvents for the experiments were purchased from commercial suppliers and used without further purification. ^{1}H NMR and ^{13}C NMR were performed on a Varian 600 MHz spectrometer. ESI-MS were acquired using a Bruker ESI-TOF. All the solutions were prepared by ultrapure water (18.2 M cm^{-1}). UV–vis absorption and fluorescence emission spectra were obtained on a Shimadzu UV-2700 spectrophotometer and a Shimadzu RF-5301 spectrofluorimeter respectively.

2.2. Preparation of the solutions and spectral measurements

The stock solution of Cys-WR (5 mM) was prepared in dimethyl sulfoxide. The solution of various testing analytes were prepared from threonine (Thr), Tyrosine (Tyr), Valine (Val), Serine (Ser), Phenylalanine (Phe), Methionine (Met), Leucine (Leu), Arginine (Arg), Histidine (His), Proline (Pro), Alanine (Ala), Glycine (Gly), isoleucine (Ile), homocysteine (Hcy), glutathione (GSH), $Fe(NO_3)_3$ (Fe^{3+}), $Al(NO_3)_3$ (Al^{3+}), $Ca(NO_3)_2$ (Ca^{2+}), $MgSO_4$ (Mg^{2+}), Na_2S (S^{2-}), $Na_2S_2O_3$ ($S_2O_3^{2-}$), Na_2SO_4 (SO_4^{2-}) in ultrapure water. The spectroscopic data was obtained in 10 mM PBS buffer solution (pH 7.4) at 25 °C. All the fluorescence spectra were performed at the excitation wavelength was 575 nm with excitation/emission slits of 5 nm.

2.3. Synthesis of Cys-WR

WR-4 was synthesized according to the previous work by Xian et al. [32]. Et_3N (230 mg, 2.27 mmol) was added to the solution of WR-4 (101 mg, 0.23 mmol) in 8 mL of dry CH_2Cl_2 at 0 °C. After stirring for 10 min, crotonyl chloride (72 mg, 0.69 mmol) was added. The mixture was sealed and stirred at room temperature for 3h. After the completion of the reaction, the resulting solution was washed with water to remove excess reactants. Next, the solution was dried over anhydrous sodium sulfate and concentrated in vacuo. The crude product was purified by column chromatography on silica gel using CH_2Cl_2: CH_3OH (100: 1) as eluent to give 60 mg of the targeted product Cys-WR (yield 51%). ^{1}H NMR (600 MHz, $CDCl_3$): δ 8.05 (d, J = 7.5 Hz, 1H), 7.66-7.62 (m, 1H), 7.59 (t, J = 7.3 Hz, 1H), 7.23-7.17 (m, 2H), 7.09 (s, 1H), 6.83 (d, J = 8.6 Hz, 1H), 6.78 (d, J = 8.6 Hz, 1H), 6.27 (s, 1H), 6.03 (d, J = 15.5 Hz, 1H), 5.78-5.73 (m, 1H), 3.61 (s, 1H), 3.48-3.43 (m, 1H), 3.34-3.31 (m, 2H), 3.14-2.93 (m, 3H), 2.69-2.63 (m, 1H), 2.15-2.06 (m, 2H), 2.01-1.96 (m, 3H), 1.51-1.41 (m, 1H), 0.93 (d, J = 6.9 Hz, 2H), 0.78 (d, J = 6.9 Hz, 1H); ^{13}C NMR (150 MHz, $CDCl_3$; values are given for one isomer with those of the second isomer in brackets): δ 169.27, 164.24, 152.48 152.37, 151.98 (151.95), 147.65 (147.64), 134.33 (134.26), 129.46, 129.04 (129.01), 125.56, 124.87, 124.72, 121.74, 116.99 (116.92), 116.84 (116.74), 110.04, 96.54 (96.42), 56.95, 50.66 (50.50), 47.65 (47.50), 45.52, 30.91 (30.19), 29.68, 23.34 (23.28), 10.10 (9.35); HR-ESI-MS m/z: $C_{31}H_{28}N_2O_5$ $[M+H]^+$ calcd for 509.2076 found 509.2076.

2.4. Cell culture and fluorescence imaging

A549 cells were grown in DMEM medium supplemented with 10% fetal bovine serum at 37 °C in an atmosphere containing 5% carbon dioxide. Firstly, the A549 cells were directly treated with Cys-WR (10 μM) for 30 min at 37 °C. Secondly, the A549 cells were pretreated with N-ethyl maleimide (NEM, 200 μM) for 60 min, and then treated with Cys-WR (10 μM) for another 30 min. Finally, the NEM (200 μM, 60 min) pretreated A549 cells were incubated with Cys (100 μM) for 30 min, and then incubated with Cys-WR (10 μM) for 30 min. All fluorescence images were obtained on an inverted fluorescence microscope (Olympus IX71, Japan) after the cells were washed with DMEM.

2.5. Fluorescence imaging in zebrafish larvae

For bioimaging in vivo, the 5-day-old zebrafish larvae were purchased from Eze-Rinka Comapany (Nanjing, China). To image endogenous Cys, the zebrafish were first directly fed with Cys-WR (10 μM) for 30 min. As a control, the zebrafish were treated with NEM (50 μM) for 60 min, further incubated with Cys-WR (10 μM) for 30 min. To image exogenous Cys, the NEM (50 μM, 60 min) pretreated zebrafish were treated with Cys (100 μM) for 60 min, further treated with Cys-WR (10 μM) for 30 min. All fluorescence images were performed on a stereomicroscope (Olympus SZX16, Japan).

3. Results and discussion

3.1. Spectra response of Cys-WR toward Cys

WR-4 was selected due to its excellent optical performance, such as NIR emission, high quantum yield and large Stokes shift (about 110 nm). Cys-WR was synthesized by two-step reactions with good yields as depicted in Fig. S3. The structure of Cys-WR was characterized by means of ^{1}H NMR, ^{13}C NMR and MS. To verify the validity of Cys-WR, the spectral sensing behavior toward Cys by UV–vis absorption and fluorescence spectroscopy was examined in PBS buffer solution (10 mM, pH 7.4). As illustrated in Fig. 1A, Cys-WR exhibited a characteristic absorption peak at 480 nm. After treatment with Cys, this peak gradually decreased and red-shifted to 543 nm. In Fig. 1B, free probe displayed weak fluorescence at 653 nm; upon the increasing concentration of Cys, the fluorescence intensity at 653 nm increased gradually and reached the approximate saturation when the concentration of Cys was 300 μM. Before and after addition of Cys, the color of probe solution turned from deep pink to brown under room light while the color of that changed from colorless to red under a portable 365 nm UV light. The reaction mechanism of Cys-WR toward Cys was confirmed by ESI-MS spectrum (Scheme 1). Addition of Cys showed the presence of two major mass peaks at m/z = 439.1658, 188.0378, corresponding to the releasing WR-4 ($[M-H]^-$) and the seven-membered cyclized by-product ($[M-H]^-$) respectively (Fig. S5).

As demonstrated in Fig. 1C, the fluorescence enhancement at 653 nm had linear relationship with the concentration of Cys ranging from 0 to 100 μM, revealing the limits of detection of 0.83 μM. For potential biological applicable, we studied the effect of pH on the fluorescence changes of the sensing system. As can be seen from Fig. 1D, no noticeable fluorescence changes were observed in the absence of Cys over a wide pH range of 4.0–9.0, suggesting the probe had a high degree of stability in the physiological pH range. When Cys was added to the solution of the probe, the fluorescence intensity increased significantly in the pH range of 6.0–9.0. Kinetics analysis of the probe was analyzed in the presence of Cys. As shown in Fig. S6, the probe in the absence of Cys was very stable. After addition of Cys, the probe reached the maximum fluorescence within 40 min. These results indicated that the probe was suitable for sensing of Cys in the physiological systems.

The specificity of Cys-WR to Cys was also investigated against other biologically relevant analyte species, such as some common amino acids (Thr, Tyr, Val, Ser, Phe, Met, Leu, Arg, His, Pro, Ala, Gly, Ile, Hcy, GSH), metal ions (Fe^{3+}, Al^{3+}, Ca^{2+}, Mg^{2+}) and anions (S^{2-}, $S_2O_3^{2-}$, SO_4^{2-}). As depicted in Fig. 1E, after addition of different possible interfering analytes to the solution of the probe, only negligible fluorescence enhancement was observed compared to Cys. Though fluorescence intensity at 653 nm of the probe increased to varying extents upon treatment with Hcy or GSH, we could still distinguish Cys from Hcy/GSH very well according to the multiple of fluorescence enhancement. Moreover, we further evaluated the specificity of the probe in the presence of co-existing analyte species (Fig. 1F). The results showed that the probe was capable of discrimination of Cys over other interfering analyte species with high selectivity and good anti-

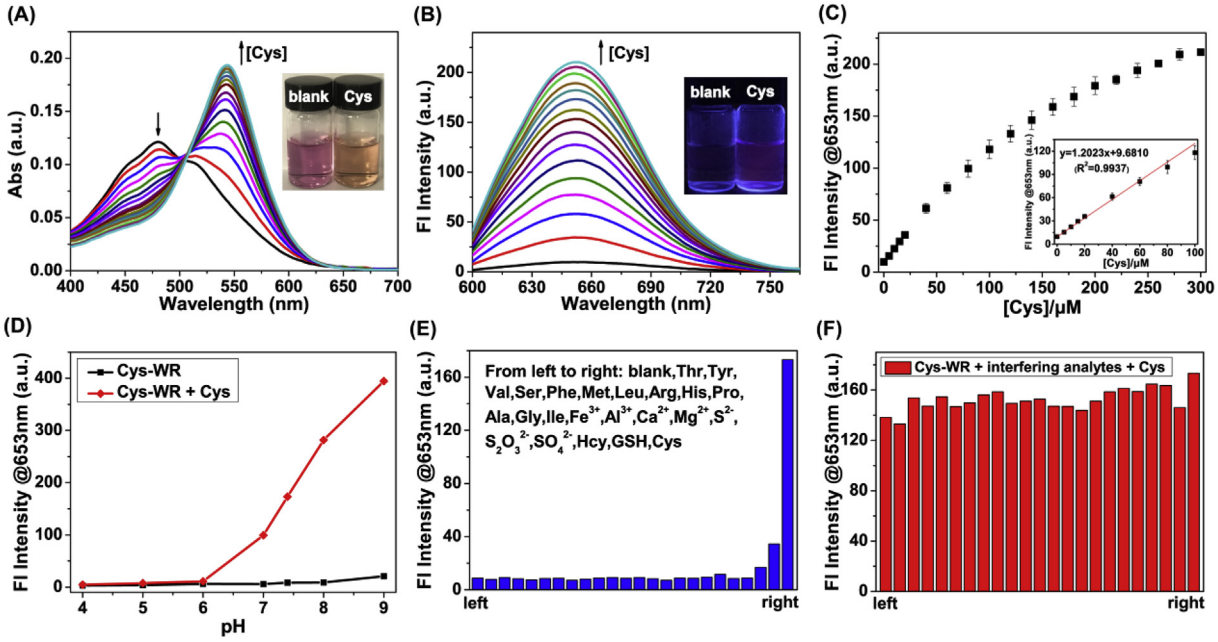

Fig. 1. UV–vis absorption (A) and fluorescence spectra (B) of probe Cys-WR (10 μM) upon gradual addition of various amounts of Cys (0–300 μM). Inset (A, B): photographs of the probe without or with Cys under room light or UV light. (C) Fluorescence intensities at 653 nm of the probe as a function of the concentration of Cys. (D) Fluorescence intensities at 653 nm of the probe in the absence or presence of 200 μM of Cys under different pH values. (E) Fluorescence response of the probe toward Cys and different interfering analytes. (F) The selectivity of Cys-WR (10 μM) toward different interfering analytes. From left to right: 200 μM for Thr, Tyr, Val, Ser, Phe, Met, Leu, Arg, His, Pro, Ala, Gly and Ile; 100 μM for Fe^{3+}, Al^{3+}, Ca^{2+}, Mg^{2+}, S^{2-}, $S_2O_3^{2-}$, SO_4^{2-}; 50 μM for Hcy; 1 mM for GSH; 200 μM for Cys.

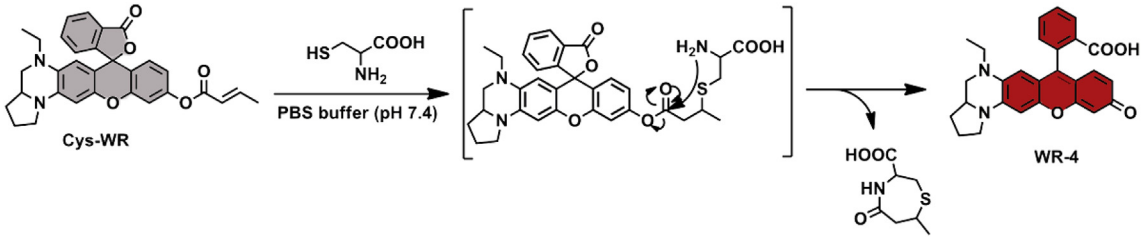

Scheme 1. Proposed sensing mechanism of Cys-WR toward Cys.

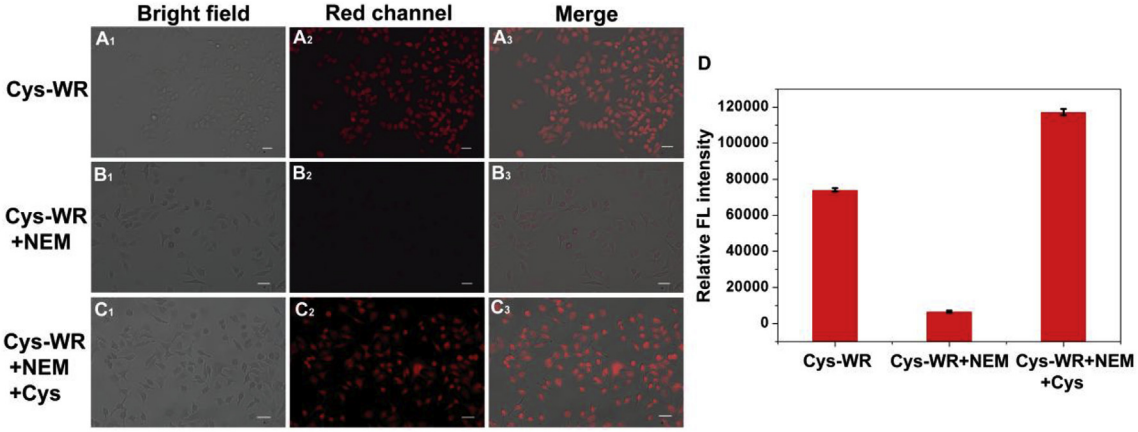

Fig. 2. Fluorescence images of A549 cells incubated with Cys-WR. (A1-A3) cells incubated with Cys-WR (10 μM) for 30 min; (B1-B3) NEM (200 μM, 60 min) pre-treated cells incubated with Cys-WR (10 μM) for 30 min; (C1-C3) NEM (200 μM, 60 min) pretreated cells incubated with Cys-WR (10 μM) for 30 min and followed by treatment with Cys (100 μM) for 30 min. (D) Relative fluorescence intensity of the corresponding fluorescence images (B1-B3). Values represent mean standard error (n = 3). Scale bar: 40 μm.

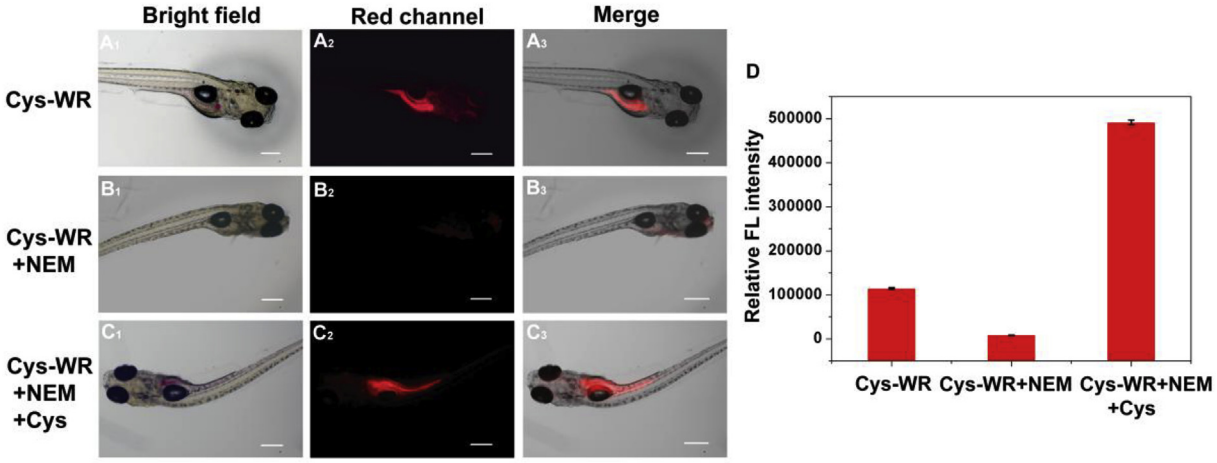

Fig. 3. Fluorescence images of zebrafish. (A1-A3) Zebrafish incubated with Cys-WR (10 μM); (B1-B3) NEM (50 μM, 60 min) pretreated zebrafish incubated with Cys-WR (10 μM) for 30 min; (C1-C3) NEM (50 μM, 60 min) pretreated zebrafish incubated with Cys-WR (10 μM) for 30 min and followed by treatment with Cys (100 μM) for 60 min. (D) Relative fluorescence intensity of the corresponding fluorescence images (B1-B3). Values represent mean standard error (n = 3). Scale bar: 200 μm.

interference ability. As a result, the designed probe Cys-WR provided a good basis for detecting Cys in complex biological systems.

3.2. Imaging of living cells

Inspired by the excellent spectral properties of probe Cys-WR, we further explored the bioimaging application of Cys-WR in vitro (Fig. 2). Prior to cellular image, the cytotoxicity of the probe was assessed by using CCK-8 assays with A549 cells. As displayed in Fig. S7, the probe was little cytotoxicity. The results showed that the probe could be applied for bioimaging. Next, the probe was employed to image endogenous and exogenous Cys in living cells under a fluorescence microscope. A549 cells incubated with the probe for 30 min elicited significant red fluorescence. As a control, when intracellular Cys were scavenged by NEM, the cells showed very weak red fluorescence. Finally, after the cells were first pretreated with NEM and subsequently treated with Cys before incubating with the probe, the strong red fluorescence was noticed. The experiment results indicated the probe was able to permeate into cells and image endogenous and exogenous Cys.

3.3. Imaging of living zebrafish larvae

The visualization of Cys in vivo was subsequently investigated using zebrafish as models. As depicted in Fig. 3, Cys-WR-loaded 5-day-old zebrafish produced strong red fluorescence from pelvic fin to pectoral fin (visceral organs region of the zebrafish). In the control experiment, the zebrafish treated with NEM before incubating with the probe resulted in a significant decrease in the red fluorescence. Additionally, when the zebrafish was pretreated with NEM, and followed by the incubation with the probe and Cys, the red fluorescence signal increased markedly. These results forcefully demonstrated that the probe was capable of sensing of Cys in vivo.

4. Conclusion

In summary, we have designed and synthesized a novel NIR off-on fluorescent probe Cys-WR with a large Stokes shift capable of Cys detection in living cells and zebrafish. The probe showed superior performance, such as NIR emission, wide linear range of 0–100 μM, high selectivity and sensitivity. Compared to most of the previous literatures, the probe could detect Cys in aqueous solution, making it more applicable to biological systems. Furthermore, the probe gave a significant fluorescence response to Cys in vitro and in vivo, which convincingly confirmed that the probe was valuable for understanding the functions of Cys in physiology and pathology.

Acknowledgement

This work was supported by the National Natural Science Foundation of China (NSFC.21602051, 21775162, 21804102), Talent Program of Hainan Medical University (Grants XRC180006), and Hundred-Talent Program (Hainan 2018).

Appendix A. Supplementary data

Supplementary data to this article can be found online at https://doi.org/10.1016/j.dyepig.2019.107722.

References

[1] Abdulle AE, van Roon AM, Smit AJ, Pasch A, van Meurs M, Bootsma H, et al. Rapid free thiol rebound is a physiological response following cold-induced vasoconstriction in healthy humans, primary Raynaud and systemic sclerosis. Phys Rep 2019;7:e14017.
[2] Zhang S, Ong CN, Shen HM. Critical roles of intracellular thiols and calcium in parthenolide-induced apoptosis in human colorectal cancer cells. Cancer Lett 2004;208:143–53.
[3] Davis W, Ronai Ze, Tew KD. Cellular thiols and reactive oxygen species in drug-induced apoptosis. J Pharmacol Exp Ther 2001;296:1–6.
[4] Chung Heaseung S, Wang SB, Venkatraman V, Murray Christopher I, Van Eyk Jennifer E. Cysteine oxidative posttranslational modifications. Circ Res 2013;112:382–92.
[5] El-Khairy L, Ueland Per M, Refsum H, Graham Ian M, Vollset Stein E. Plasma Total cysteine as a risk factor for vascular disease. Circulation 2001;103:2544–9.
[6] Jacob N, Bruckert E, Giral P, Foglietti MJ, Turpin G. Cysteine is a cardiovascular risk factor in hyperlipidemic patients. Atherosclerosis 1999;146:53–9.
[7] Qu W, Niu C, Zhang X, Chen W, Yu F, Liu H, et al. Construction of a novel far-red fluorescence light-up probe for visualizing intracellular peroxynitrite. Talanta 2019;197:431–5.
[8] Liu H, Radford MN, Yang CT, Chen W, Xian M. Inorganic hydrogen polysulfides: chemistry, chemical biology and detection. Br J Pharmacol 2019;176:616–27.
[9] He N, Bai S, Huang Y, Xing Y, Chen L, Yu F, et al. Evaluation of glutathione S-transferase inhibition effects on idiopathic pulmonary fibrosis therapy with a near-infrared fluorescent probe in cell and mice models. Anal Chem 2019;91:5424–32.
[10] Chen W, Pacheco A, Takano Y, Day JJ, Hanaoka K, Xian M. A single fluorescent probe to visualize hydrogen sulfide and hydrogen polysulfides with different fluorescence signals. Angew Chem Int Ed 2016;55:9993–6.
[11] Chen W, Rosser EW, Matsunaga T, Pacheco A, Akaike T, Xian M. The development of fluorescent probes for visualizing intracellular hydrogen polysulfides. Angew Chem Int Ed 2015;54:13961–5.
[12] Ning J, Liu T, Dong P, Wang W, Ge G, Wang B, et al. Molecular design strategy to construct the near-infrared fluorescent probe for selectively sensing human cytochrome P450 2J2. J Am Chem Soc 2019;141:1126–34.
[13] Huang Y, Zhang X, He N, Wang Y, Kang Q, Shen D, et al. Imaging of anti-inflammatory effects of HNO via a near-infrared fluorescent probe in cells and in rat gouty arthritis model. J Mater Chem B 2019;7:305–13.

[14] Wu D, Chen L, Lee W, Ko G, Yin J, Yoon J. Recent progress in the development of organic dye based near-infrared fluorescence probes for metal ions. Coord Chem Rev 2018;354:74–97.
[15] Reineck P, Gibson BC. Near-infrared fluorescent nanomaterials for bioimaging and sensing. Adv Opt Mater 2017;5:1600446.
[16] Yin CX, Xiong KM, Huo FJ, Salamanca JC, Strongin RM. Fluorescent probes with multiple binding sites for the discrimination of Cys, Hcy, and GSH. Angew Chem Int Ed 2017;56:13188–98.
[17] Zhu D, Yan X, Ren A, Xie W, Duan Z. A novel colorimetric and ratiometric fluorescent probe for cysteine based on conjugate addition-cyclization-elimination strategy with a large Stokes shift and bioimaging in living cells. Anal Chim Acta 2019;1058:136–45.
[18] Wang N, Chen M, Gao J, Ji X, He J, Zhang J, et al. A series of BODIPY-based probes for the detection of cysteine and homocysteine in living cells. Talanta 2019;195:281–9.
[19] Zhang X, He N, Huang Y, Yu F, Li B, Lv C, et al. Mitochondria-targeting near-infrared ratiometric fluorescent probe for selective imaging of cysteine in orthotopic lung cancer mice. Sensors Actuat B Chem 2019;282:69–77.
[20] Jia X, Niu C, He Y, Sun Y, Liu H. A hybrid coumarin-semifluorescein-based fluorescent probe for the detection of cysteine. J Fluoresc 2018;28:1059–64.
[21] Yue Y, Huo F, Ning P, Zhang Y, Chao J, Meng X, et al. Dual-site fluorescent probe for visualizing the metabolism of Cys in living cells. J Am Chem Soc 2017;139:3181–5.
[22] Yue Y, Huo F, Li X, Wen Y, Yi T, Salamanca J, et al. pH-dependent fluorescent probe that can be tuned for cysteine or homocysteine. Org Lett 2017;19:82–5.
[23] Qiu X, Jiao X, Liu C, Zheng D, Huang K, Wang Q, et al. A selective and sensitive fluorescent probe for homocysteine and its application in living cells. Dyes Pigments 2017;140:212–21.
[24] Nawimanage RR, Prasai B, Hettiarachchi SU, McCarley RL. Cascade reaction-based, near-infrared multiphoton fluorescent probe for the selective detection of cysteine. Anal Chem 2017;89:6886–92.
[25] Li SJ, Fu YJ, Li CY, Li YF, Yi LH, Ou YJ. A near-infrared fluorescent probe based on BODIPY derivative with high quantum yield for selective detection of exogenous and endogenous cysteine in biological samples. Anal Chim Acta 2017;994:73–81.
[26] Fu ZH, Han X, Shao Y, Fang J, Zhang ZH, Wang YW, et al. Fluorescein-based chromogenic and ratiometric fluorescence probe for highly selective detection of cysteine and its application in bioimaging. Anal Chem 2017;89:1937–44.
[27] Fan W, Huang X, Shi X, Wang Z, Lu Z, Fan C, et al. A simple fluorescent probe for sensing cysteine over homocysteine and glutathione based on PET. Spectrochim Acta Mol Biomol Spectros 2017;173:918–23.
[28] Ji Y, Dai F, Zhou B. Developing a julolidine-fluorescein-based hybrid as a highly sensitive fluorescent probe for sensing and bioimaging cysteine in living cells. Talanta 2019;197:631–7.
[29] Zhang M, Wang L, Zhao Y, Wang F, Wu J, Liang G. Using bioluminescence turn-on to detect cysteine in vitro and in vivo. Anal Chem 2018;90:4951–4.
[30] Ren X, Tian H, Yang L, He L, Geng Y, Liu X, et al. Fluorescent probe for simultaneous discrimination of Cys/Hcy and GSH in pure aqueous media with a fast response under a single-wavelength excitation. Sensors Actuat B Chem 2018;273:1170–8.
[31] Wang Q, Wang H, Huang J, Li N, Gu Y, Wang P. Novel NIR fluorescent probe with dual models for sensitively and selectively monitoring and imaging Cys in living cells and mice. Sensors Actuat B Chem 2017;253:400–6.
[32] Chen W, Xu S, Day JJ, Wang D, Xian M. A general strategy for development of near-infrared fluorescent probes for bioimaging. Angew Chem Int Ed 2017;56:16611–5.